

Enhanced quantum tunneling in quantum Zeno dynamics freezing momentum direction

Miguel A. Porras

Grupo de Sistemas Complejos, ETSIME, Universidad Politécnica de Madrid, Rios Rosas 21, 28003 Madrid, Spain

Nilo Mata

*Departamento de Energía y Combustibles, ETSIME,
Universidad Politécnica de Madrid, Rios Rosas 21, 28003 Madrid, Spain*

Isabel Gonzalo

*Departamento de Óptica, Facultad de Ciencias Físicas,
Universidad Complutense de Madrid, Ciudad Universitaria s/n, 28040 Madrid, Spain*

Quantum tunneling (QT) and its control is of great importance in many natural phenomena such as nuclear fusion, nucleosynthesis in general, high-energy particle collisions, or electron and proton transfer in chemical and biochemical processes. The QT probability of a particle is seen here to be enhanced up to unity via the so-called quantum Zeno dynamics undergone by a particle directed towards a potential barrier while the momentum direction of the particle is frequently monitored.

To explain the quantum Zeno effect (QZE) it is often said that “a watched pot never boils”. Frequent measurements that ascertain whether a quantum system remains in its initial state slow down its evolution. The QZE has been known for almost a century [1], was given its name after [2], and has been observed in diverse physical systems [3, 4]. The simplest manifestations take place in quantum two-level systems; for example, the inhibition of decay of an unstable state [3], or inhibition of quantum tunneling (QT) in a double-well potential [5, 6]. If the repeated measurements are faster than the short-term parabolic transition probability characteristic of Schrödinger evolution, decay or QT become less probable, and impossible with a continuous of measurements. Still, the QZE or “paradox” is not exempt of controversies, also in the double-well with different models of measurement [7–10].

A generalization of the QZE is quantum Zeno dynamics (QZD) [11]. The frequent measurements of an observable of the system ascertain here whether the state of the system is in a multidimensional subspace of the system’s Hilbert space [12]. In QZD, the remaining or concomitant QZE (in the sense of freezing the evolution) is more subtle: what tends to be frozen is the transition from the multidimensional subspace defined by the measurements to the complementary subspace, but the system continues to evolve coherently within each subspace [13]. QZD has recently been observed in a rubidium condensate, where a superselection rule between two- and three-dimensional subspaces arises [14].

QZD becomes more involved in an infinite-dimensional Hilbert space [12], as that of a simple moving particle. In all previous analysis the measurements involve position measurements, which, being necessarily imprecise, are aimed to ascertain the location in a region of space, say Δx . Ref. [15] provides a theoretical demonstration that the QZD in the limit of continuous, selective measurements of position, modeled as von Newmann projec-

tions, becomes a unitary evolution confined in the Hilbert subspace defined by Δx with hard, Dirichlet boundary conditions. Below the limit of continuous measurements, a free particle—the Zeno arrow—is seen to tend to stop in Δx in a quantum-cat-state of the particle moving forward and backward at the same time [16]. In [17], computer simulations of QZD (although it is called QZE) with measurements of position, modeled either as nonselective projections or pointer measurements, are also be seen to freeze the particle.

To our knowledge, the complementary QZD with momentum in place of position measurements has not been addressed, although such QZD could strongly affect the dynamics of particles subject to forces, the most immediate being QT through a potential barrier. We show that repeated measurements that would ascertain whether the momentum is in a region of momentum space, tend to freeze the momentum. To the purpose of QT, it turns out that repeated measurements that simply determine the direction of momentum (positive or negative in our one-dimensional geometry) suffice for the direction to freeze, and therefore for the particle to pass the barrier.

In line with [15, 16], we first adopt an operational approach to measurements as selective von Newmann projections. For a particle launched towards positive x , only the possibility that the momentum is positive in all measurements is considered. Its simplicity allows us to simulate the effect of high enough number of measurements with which the QT probability approaches unity. Next we move to a more physical model of measurement as a nonselective interaction with a probe particle to which information on the direction of the particle is transferred, and reduces the state of the particle to a mixture of states with opposite momenta [18–20]. In this picture, all possibilities that the momentum is positive at the last measurement are considered. The measurements as interactions also cause the direction to freeze, and the particle to tunnel, with a probability higher than with the selec-

tive measurements, and therefore also approaching unity as their frequency increases, pointing to the emergence of a superselection rule between Hilbert's subspaces of different momenta.

Contrary to QZE-induced QT inhibition of bounded states in a double-well by measuring well occupation, QZD with momentum measurements of unbounded states promotes QT. As such, relevant related phenomena would be those where enhancement of QT will have an impact, such as enhancing the efficiency of nuclear fusion and other nucleosynthesis processes, facilitating nucleus-nucleus collisions in particle colliders [21], as an additional tool to QT for the control of chemical reactivity [22] in, e.g., electron and proton transfer in chemical and biochemical processes [23].

We then consider a particle of mass m , wave function $\psi(x, t = 0) = \psi(x) \exp(ik_0 x)$ well-within the half-space $x < 0$, and positive mean momentum $p_0 = \hbar k_0$ such that the mean kinetic energy $E_c = p_0^2/2m$ is smaller than the peak potential energy V_0 of a barrier $V(x)$ localized about $x = 0$. For concreteness we will use $V(x) = V_0/(1+|x/b|^m)$, where b measures the half-width of the barrier, and $m > 0$ ($m \rightarrow \infty$ is a square barrier), but the results are qualitatively the same for other forms of barrier. For a well-directed particle translation dominates over wave packet spreading, implying that p_0 is larger than its uncertainty, Δp . We rewrite Schrödinger equation,

$$i\hbar \frac{\partial \psi}{\partial t} = -\frac{\hbar^2}{2m} \frac{\partial^2 \psi}{\partial x^2} + V\psi, \quad (1)$$

using the dimensionless spatial coordinate $\xi = x/(\hbar/\Delta p)$ (x in units of the wave function width $\Delta x \sim \hbar/\Delta p$) and dimensionless time $\tau = t/(2m\Delta x/p_0) = t/(2\hbar m/\Delta pp_0)$ (time in units of the time taken for the particle to traverse its own wave function), as

$$i \frac{\partial \psi}{\partial \tau} = -\frac{1}{\kappa_0} \frac{\partial^2 \psi}{\partial \xi^2} + \kappa_0 v_0 v \psi, \quad (2)$$

where $v = 1/(1+|\xi/\xi_b|^m)$, and ξ_b is the potential width in units of the wave function width. The parameters at work in the QT dynamics are then $v_0 = V_0/E_c$ and $\kappa_0 = p_0/\Delta p$. The situation of interest is that with $v_0 > 1$ (QT) and $\kappa_0 > 1$ (well-directed particle).

We consider the QZD of the particle subjected to frequent measurements that ascertain whether the momentum is in a certain interval of momentum space or not. In the context of QT, the QZD turns out to be qualitatively similar if this interval is Δp , any other interval about p_0 , or is simply positive.

In a first approach, the measurements are operationally summarized as projections of the state onto the subspace of positive momenta. These measurements are selective, i.e., meaning that we only consider the event that the momentum is positive in all the measurements. This would be the situation with a measuring device that eliminates the particle upon a negative outcome. In the standard Zeno scheme, the particle evolves according to (2) during a certain total time τ_{\max} , while the evolution is N

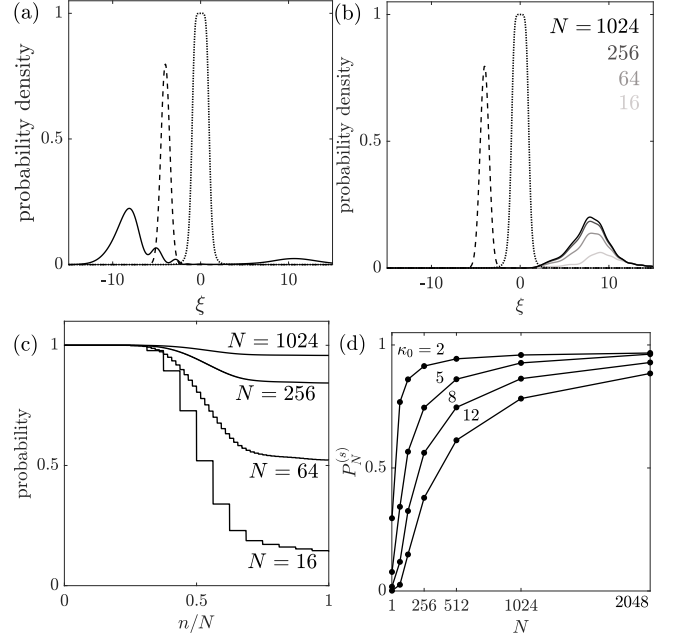


FIG. 1. (a) Partially transmitted and reflected probability density (solid curves) at time $\tau_{\max} = 6.24$ for the input wave packet $\psi = (2/\pi)^{1/4} \exp[-(\xi - \xi_0)^2] \exp(i\kappa_0 \xi)$ ($\kappa_0 = 4$, $\xi_0 = -4$) at $\tau = 0$ (dashed curve) through the barrier of width $\xi_b = 1$, $m = 6$ and height $v_0 = 1.5$ (dash-dotted curve) without any measurement. Tunneling probability is $P_1^{(s)} = 0.162$. (b) The same but with $N = 2^4, 2^6, 2^8$ and 2^{10} measurements between $\tau = 0$ and τ_{\max} yielding respective tunneling probabilities $P_N^{(s)} = 0.31, 0.69, 0.90$, and 0.97 . The weak reflected wave is eliminated by the projections. (c) Probability that the direction remains positive at the n th measurement, for different values of N . (d) Tunneling probability as a function of N for several values of κ_0 .

times interrupted to monitor the direction of movement. The projective measurements are performed at the times $\tau_n = n\tau_{\max}/N$, $n = 1, 2 \dots N$ equispaced $\Delta\tau = \tau_{\max}/N$. E.g., after $n-1$ positive measurements, the wave function ψ_{n-1} evolves to ψ_n according to the Schrödinger equation (2), and at the n positive measurement experiences the projection $\hat{\psi}_n(\kappa, \tau_n) \rightarrow \hat{\psi}_{n,\text{meas}}(\kappa, \tau_n) = \hat{\psi}_n(\kappa, \tau_n) \theta(\kappa)$, where $\hat{\psi}_n(\kappa, \tau_n)$ is the wave function in momentum space, $\theta(\kappa)$ is the Heaviside step function, and $\kappa = p/\Delta p$ is the dimensionless momentum. *Stricto sensu*, one should normalize the wave function after each measurement, but in a problem involving many measurement it is simpler to use the unnormalized wave functions $\hat{\psi}_{n,\text{meas}}(\kappa, \tau_n)$ whose norm is the probability that the momentum of the particle continues to be positive after the n measurement. In particular, after the N measurement at time τ_{\max} , the probability that all outcomes were positive is the norm

$$P_N^{(s)} = \int_{-\infty}^{\infty} |\hat{\psi}_{N,\text{meas}}(\kappa, \tau_{\max})|^2 d\kappa \quad (3)$$

of $\hat{\psi}_{N,\text{meas}}(\kappa, \tau_{\max})$ (the lower limit can obviously be set

to zero).

We choose the initial position at $\tau = 0$ such that the barrier does not yet affect the particle, and the time τ_{\max} such that the transmission/reflection process is completed, with or without measurements. For a particle launched from the left, the probability of finding the particle to the right of the barrier, $P_+^{(s)} = \int_0^\infty |\psi(\xi, \tau_{\max})|^2 d\xi$, at τ_{\max} must coincide with the probability $P_N^{(s)}$ that the momentum is positive. With a single measurement, $P_1^{(s)}$ yields the standard QT probability.

In the example of Fig. 1(a), the QT probability is $P_1 = 0.162$ (all numerical simulations of Schrödinger equation in this Letter are performed with a standard Fourier split-step method with a fast Fourier transform algorithm). Figure 1(b) evidences that monitoring more and more frequently whether the direction remains positive increases the QT probability by freezing the momentum direction. To illustrate how the increasing tunneling probability $P_N^{(s)}$ is furnished from one to the next measurement, Fig. 1(c) represents the decreasing norm of the wave function as the measurements are performed, that is, the probability that the direction remains positive after the n th measurement. The more measurements there are (more steps down), the higher $P_N^{(s)}$ (less you go down). The QT probability $P_N^{(s)}$ is represented as a function of N in Fig. 1(d) for different values of κ_0 . As $\kappa_0 \rightarrow \infty$, the QT probability without measurements ($P_1^{(s)}$) tends to zero, which, given the fixed value of the barrier height $v_0 > 1$, can be regarded as the classical limit. The QT probability tends always to unity, but it needs more measurements as κ_0 increases.

These results motivate us to formulate the same problem using a more physical model of the measurement process [18–20], which in turn could shed light on how they could be implemented in practice. Each measurement is modelled as a short interaction with an environmental particle, or probe, to which information on the direction of the particle is transferred. Upon tracing over the probe states after the interaction, the positive and negative parts of the wave function decohere. As probe particles, one could imagine, for instance, photons travelling collinear with the particle that are red or blue Doppler-shifted upon backscattering by the particle, depending on whether the particle travels forward or backward. These type of interactions discriminate the two directions but do not select a particular outcome.

With the same QZD scheme, the initial pure state $|\psi_0\rangle$ evolves to $|\psi_1\rangle = e^{-iH\Delta\tau}|\psi_0\rangle$, with $H = (-1/\kappa_0)\partial^2\psi/\partial\xi^2 + \kappa_0 v_0 v(\xi)$, in a first time interval $\Delta\tau$. Under the action of the potential barrier and wave packet spreading, $|\psi_1\rangle$ may have acquired positive and negative momenta and hence can always be written as the superposition $|\psi_1\rangle = |\psi_{1,+}\rangle + |\psi_{1,-}\rangle$ of the orthogonal states

$$|\psi_{1,+}\rangle = \int_0^\infty d\kappa \hat{\psi}_1(\kappa) |\kappa\rangle, \quad |\psi_{1,-}\rangle = \int_{-\infty}^0 d\kappa \hat{\psi}_1(\kappa) |\kappa\rangle. \quad (4)$$

As above, we do not write $|\psi_1\rangle = a_+|\psi_{1,+}\rangle' + a_-|\psi_{1,-}\rangle'$ with normalized $|\psi_{1,\pm}\rangle'$, but the norms of $|\psi_{1,\pm}\rangle$, $\langle\psi_{1,\pm}|\psi_{1,\pm}\rangle = |a_\pm|^2$, give the respective probabilities of realization.

Interaction with the probe, whose initial state is $|\chi\rangle$, leads to the transitions $|\psi_{1,\pm}\rangle|\chi\rangle \rightarrow |\psi_{1,\pm}\rangle|\chi_\pm\rangle$ of the particle-probe system. Discrimination between positive or negative momenta of the particle requires the states $|\chi_+\rangle$ and $|\chi_-\rangle$ of the probe to be orthonormal. For the state $|\psi_1\rangle$ at $\Delta\tau$, the result of the interaction is the entangled state $|\psi_{1,+}\rangle|\chi_+\rangle + |\psi_{1,-}\rangle|\chi_-\rangle$, whose density matrix is

$$\rho_{1,\text{meas}} = (|\psi_{1,+}\rangle|\chi_+\rangle + |\psi_{1,-}\rangle|\chi_-\rangle) \times (\langle\psi_{1,+}| \langle\chi_+| + \langle\psi_{1,-}| \langle\chi_-|), \quad (5)$$

and, if only the particle is considered after separation of the probe, its reduced density matrix is obtained by tracing over the probe:

$$\rho_{1,\text{red}} = \langle\chi_+|\rho_{\text{meas}}|\chi_+\rangle + \langle\chi_-|\rho_{\text{meas}}|\chi_-\rangle = |\psi_{1,+}\rangle\langle\psi_{1,+}| + |\psi_{1,-}\rangle\langle\psi_{1,-}|, \quad (6)$$

which is a mixture of a particle travelling forward or backward with probabilities $\langle\psi_{1,\pm}|\psi_{1,\pm}\rangle$.

The particle is next left to evolve another time $\Delta\tau$ to $\rho_2 = e^{-iH\Delta\tau}\rho_{1,\text{red}}e^{iH\Delta\tau}$, that is,

$$\rho_2 = e^{-iH\Delta\tau}|\psi_{1,+}\rangle\langle\psi_{1,+}|e^{iH\Delta\tau} + e^{-iH\Delta\tau}|\psi_{1,-}\rangle\langle\psi_{1,-}|e^{iH\Delta\tau}, \quad (7)$$

where, as before, $e^{-iH\Delta\tau}|\psi_{1,+}\rangle \equiv |\psi_{2,+}\rangle = |\psi_{2,++}\rangle + |\psi_{2,+-}\rangle$ and $e^{-iH\Delta\tau}|\psi_{1,-}\rangle \equiv |\psi_{2,-}\rangle = |\psi_{2,-+}\rangle + |\psi_{2,--}\rangle$, since, again, any of these states may acquire opposite momenta. Here, also as above,

$$|\psi_{2,++}\rangle = \int_0^\infty d\kappa \hat{\psi}_{2,+}(\kappa) |\kappa\rangle, \quad |\psi_{2,+-}\rangle = \int_{-\infty}^0 d\kappa \hat{\psi}_{2,+}(\kappa) |\kappa\rangle, \\ |\psi_{2,-+}\rangle = \int_0^\infty d\kappa \hat{\psi}_{2,-}(\kappa) |\kappa\rangle, \quad |\psi_{2,--}\rangle = \int_{-\infty}^0 d\kappa \hat{\psi}_{2,-}(\kappa) |\kappa\rangle.$$

The density matrix is then written as

$$\rho_2 = (|\psi_{2,++}\rangle + |\psi_{2,+-}\rangle)(\langle\psi_{2,++}| + \langle\psi_{2,+-}|) + (|\psi_{2,-+}\rangle + |\psi_{2,--}\rangle)(\langle\psi_{2,-+}| + \langle\psi_{2,--}|), \quad (8)$$

and in a second interaction with a probe ($|\psi_{2,\dots\pm}\rangle|\chi\rangle \rightarrow |\psi_{2,\dots\pm}\rangle|\chi_\pm\rangle$) the density matrix of the particle-probe system is

$$\rho_{2,\text{meas}} = (|\psi_{2,++}\rangle|\chi_+\rangle + |\psi_{2,+-}\rangle|\chi_-\rangle) \times (\langle\psi_{2,++}| \langle\chi_+| + \langle\psi_{2,+-}| \langle\chi_-|) + (|\psi_{2,-+}\rangle|\chi_+\rangle + |\psi_{2,--}\rangle|\chi_-\rangle) \times (\langle\psi_{2,-+}| \langle\chi_+| + \langle\psi_{2,--}| \langle\chi_-|). \quad (9)$$

Tracing over the probe after the interaction, the reduced density matrix of the particle is

$$\rho_{2,\text{red}} = |\psi_{2,++}\rangle\langle\psi_{2,++}| + |\psi_{2,+-}\rangle\langle\psi_{2,+-}| + |\psi_{2,-+}\rangle\langle\psi_{2,-+}| + |\psi_{2,--}\rangle\langle\psi_{2,--}|, \quad (10)$$

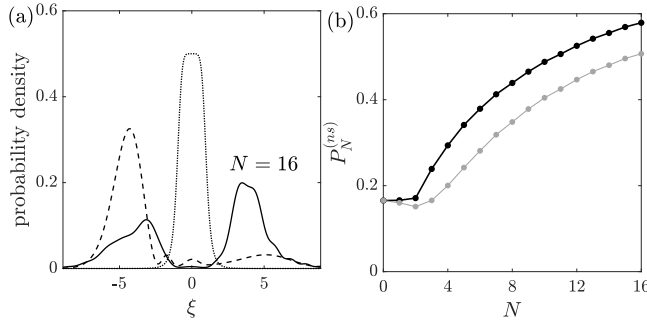


FIG. 2. (a) Partially transmitted and reflected probability density at time $\tau_{\max} = 3.56$ for the input wave packet $\psi = (2/\pi)^{1/4} \exp[-(\xi - \xi_0)^2] \exp(i\kappa_0\xi)$ ($\kappa_0 = 4$, $\xi_0 = -2.67$) at $\tau = 0$ through the barrier of width $\xi_b = 1$, $m = 6$ and height $v_0 = 1.5$ without any measurement (dashed curve), and the same with $N = 16$ measurements (solid curve). To concentrate the measurements, 15 of them are performed between $\tau_1 = 0.88$ and $\tau_2 = 3$, and the last one at τ_{\max} . QT probability without measurements is $P_1^{(ns)} = 0.162$, and with $N = 16$ measurements is $P_{16}^{(ns)} = 0.579$. (b) QT probability as a function of N when measurements are nonselective (black curve) and selective (gray curve), for comparison.

which is a mixture of four states of all possible outcomes in the two measurements with norms equal to the probabilities of realization.

This procedure is repeated up to N times, whereby a mixture of 2^N states, e.g., $|\psi_{N,++-++-+}\rangle$, (the number of plus and minus signs is N) corresponding to all possible outcomes in each of the N measurements, is obtained, whose norms are their respective probabilities or realization. Among them, there are 2^{N-1} states yielding positive direction at the last measurement. Thus, the probability that the direction of the particle is positive at the N measurement is the sum of their respective probabilities:

$$P_N^{(ns)} = \sum_{-N}^{2^N-1} \langle \psi_{N,\dots} | \psi_{N,\dots} \rangle = \sum_{-N}^{2^N-1} \int_{-\infty}^{\infty} |\hat{\psi}_{N,\dots}(\kappa)|^2 d\kappa \quad (11)$$

(again the lower limit can be set to zero). Note that the term with N positive signs is the probability that all outcomes were positive and therefore coincides with $P_N^{(s)}$ in (3). We then conclude that these interactions of the particle with probe particles discriminating the particle direction also result in freezing the direction, and their efficiency is higher than with selective measurements.

If, for brevity we call each incoherent state at the N th measurement $|\psi_{N,i}\rangle$, the probability density of finding the particle at ξ is $\langle \xi | \rho_{N,\text{red}} | \xi \rangle = \sum_i |\langle \xi | \psi_{N,i} \rangle|^2 = \sum_i |\psi_{N,i}(\xi)|^2$, verifying $\int_{-\infty}^{\infty} \langle \xi | \rho_{N,\text{red}} | \xi \rangle d\xi = 1$ since temporal evolution and measurements are unitary transformations. For a particle initially located well-before

the barrier, and with a sufficiently long time τ_{\max} , the probability that the particle is to the right of the barrier,

$$P_+^{(ns)} = \int_0^{\infty} \langle \xi | \rho_{N,\text{red}} | \xi \rangle d\xi = \sum_i \int_0^{\infty} |\psi_{N,i}(\xi)|^2 d\xi, \quad (12)$$

must coincide with $P_N^{(ns)}$, implying also an enhanced QT probability.

We have implemented the above procedure on a computer and relevant results are depicted in Fig. 2. Note that the number of times Schrödinger equation (2) is to be solved with N measurements is 2^0 up to the first measurement, 2^1 up to the second, and so on, i.e., $\sum_{n=0}^N 2^n = 2^{N+1} - 1$, which grows exponentially and limits the maximum number of measurements to a few tens in our computer facility. Given the difficulty of simulating a high number of measurements, and that they have no effect on the freely moving particle before and after the barrier, the N measurements between $\tau = 0$ and τ_{\max} are concentrated in $N - 1$ measurements in a shorter time interval $[\tau_1, \tau_2]$ in which the wave function significantly overlaps the potential, plus the N measurement at τ_{\max} for the reflection/transmission process to be concluded. The interval $[\tau_1, \tau_2]$ is the same for all N , so that increasing N is the same as increasing the frequency. Under the conditions specified in the caption, Fig. 2(a) shows the spatial probability densities with $N = 1$, with QT probability $P_1^{(ns)} = 0.162$, and with $N = 16$ measurements, with QT probability $P_{16}^{(ns)} = 0.579$. The plot of $P_N^{(ns)}$ versus N in Fig. 2(b) evidences the increasing probability that the momentum direction is frozen Zeno effect, and hence the increasing QT probability. Since $P_N^{(s)}$ (gray curve) approaches unity, $P_N^{(ns)}$ (black curve) does faster.

To conclude, we have unveiled and described the existence of a quantum mechanical dynamics of a particle—a quantum Zeno dynamics involving frequent measurements of momentum direction—that deeply affect quantum tunneling up to the point of ensuring transmission. In addition to its theoretical interest, and given the enormous technological developments in, for example, ultrafast optical metrology, it is not unreasonable to think that this dynamics could be implemented in practice. “Zeno-assisted tunneling” would have an impact in the diverse natural phenomena where quantum tunneling is a key player.

M.A.P. acknowledges support from Project No. PGC2018-093854-B-I00, and M.A.P. and I.G. from project No. FIS2017-87360-P of the Spanish Ministerio de Ciencia, Innovación y Universidades. N.M. acknowledges support from grant No. D480 (Beca de colaboración de formación) of the Universidad Politécnica de Madrid.

[1] J. von Neumann, *Die Mathematische Grundlagen der Quantenmechanik* (Berlin, Springer 1932).

[2] B. Misra and E.C.G. Sudarshan, “The Zeno’s paradox in quantum theory,” *J. Math. Phys.* **18** 756 (1977).

[3] W.M. Itano, D.J. Heinzen, J.J. Bollinger, and D.J. Wineland, “Quantum Zeno effect,” *Phys. Rev. A* **41** 2295 (1990).

[4] M.C. Fischer, B. Gutiérrez-Medina, and M. G. Raizen, “Observation of the Quantum Zeno and Anti-Zeno Effects in an Unstable System,” *Phys. Rev. Lett.* **87**, 040402 (2001).

[5] T.P. Altenmuller and A. Schenzle, “Quantum Zeno effect in a double-well potential: A model of a physical measurement,” *Phys. Rev. A* **49**, 2016 (1994).

[6] L Lerner *Eur. J. Phys.* “The quantum Zeno effect in double well tunnelling,” **39**, 035407 (2018).

[7] H. Fearn and W. E. Lamb, Jr. “Computational approach to the quantum Zeno efect: Position measurements,” *Phys. Rev. A* **46**, 1199 (1992).

[8] D. Home and M.A.B. Whitaker, “Comment on ‘Computational approach to the quantum Zeno effect: Position measurements’,” *Phys. Rev. A* **48**, 2502 (1993).

[9] J. Ruseckas and B. Kaulakys, “Real measurements and the quantum Zeno effect,” *Phys. Rev. A* **63**, 062103 (2001).

[10] A.D. Godbeer, J.S. Al-Khalili, and P.D. Stevenson, “Environment-induced dephasing versus von Neumann measurements in proton tunneling,” *Phys. Rev. A* **90**, 012102 (2014).

[11] P. Facchi, V. Gorini, G. Marmo, S. Pascazio, and E.C.G. Sudarshan, “Quantum Zeno dynamics,” *Phys. Lett. A* **275**, 12-19 (2000).

[12] P. Facchi and S. Pascazio *J. Phys. A: Math. Theor.* **41**, 493001 (2008).

[13] P. Facchi and S. Pascazio, “Quantum Zeno Subspaces,” *Phys. Re. Lett.* **89**, 080401 (2002).

[14] F. Schäfer, I. Herrera, S. Cherukattil, C. Lovecchio, F.S. Cataliotti, F. Caruso, and A. Smerzi, “Exprimental realization of quantum Zeno dynamics,” *Nature. Comm.* **5**, 3194 (2014).

[15] P. Facchi, S. Pascazio, A. Scardicchio, and L. S. Schulman, “Zeno dynamics yields ordinary constraints,” *Phys. Rev. A* **65**, 012108 (2001).

[16] M.A. Porras, A. Luis, and I. Gonzalo, “Quantum Zeno effect for a free-moving particle,” *Phys. Rev. A* **90**, 062131 (2014).

[17] D. Wallace, “Simple computer model for the quantum Zeno effect,” *Phys. Rev. A* **63**, 022109 (2001).

[18] M. Simonius, “Spontaneous Symmetry Breaking and Blocking of Metastable States,” *Phys. Rev. Lett.* **40**, 980 (1977).

[19] W.H. Zurek, “Pointer basis of quantum apparatus: Into what mixture does the wave packet collapse?,” *Phys. Rev. D* **24**, 1516 (1981).

[20] M.B. Mensky, *Quantum Measurements and Decoherence. Models and Phenomenology*, Fundamental Theories of Physics **110**, (Springer-Science+Business Media, B.Y., 2000).

[21] C.A. Salgado *et al*, “Proton–nucleus collisions at the LHC: Scientific opportunities and requirements,” *J. Phys. G: Nucl. Part. Phys.* **39**, 015010 (2012).

[22] P.R. Schreiner, “Tunneling Control of Chemical Reactions: The Third Reactivity Paradigm,” *J. Am. Chem. Soc.* **139** (43), 15276 (2017).

[23] G.R. Fleming, G.D. Scholes, and Y.-C. Cheng, “Quantum effects in biology,” *Procedia Chemistry* **3**, 38 (2011).